# Utilization of Calcined Sandstone and Calcined Laterite as an Adsorbent for the Removal of Arsenic from Water

N'Da Akoua Alice Koua-Koffi[1*]     Lassina Sandotin Coulibaly [12]

Lydie Clarisse Mangoua-Allali[1]     Lacina Coulibaly[12]

1.Nangui Abrogoua, Laboratoire Environnement et Biologie Aquatique (LEBA) 02 B.P. 802 Abidjan 02, Côte d'Ivoire

2.Université de Man, Département de Géologie et Matériaux B.P.V. 40 Man, Côte d'Ivoire

**Abstract**

Calcined sandstone and calcined laterite were tested as adsorbent at a low cost for the removal of arsenic (As) from the drinking water. The natural materials were collected in Côte d'Ivoire, washed and then dried at a temperature of 60 ° C and finally calcined in an oven at the atmospheric air in several temperatures 300 ° C, 400 ° C, 500 ° C, 600 ° C and 700 ° C. The study of adsorption of the arsenic was realized for the various adsorbates. It showed that the biggest efficiency of the elimination was attributed to the calcined sandstone to 300°C and 400°C for laterite during 2h with a percentage that reached 99.4 %. At this calcination temperature, amount of arsenic in treated water, satisfying the World Health Organization (WHO) standard for drinking water at initial arsenic concentrations greater than 5 mg/L. The chemical composition of the obtained adsorbs was analyzed by X-ray diffraction, Fourier transform infrared spectroscopy (FTIR) and thermal analysis (TGA-DSC). Adsorption has been described by the pseudo-second-order model. Calcination of sandstone and laterite increases the adsorption of arsenic on the materials.

**Keywords**: Arsenic, calcined sandstone, calcined laterite, adsorption, temperature.

## 1. Introduction

Elevated concentration of arsenic (As) in soil and groundwater arising from both natural (Fields *et al*., 2000) source and anthropogenic activities are reported in several countries around the world (Welté & Montiel, 2004). Ingestion of arsenic leads to abdominal pain, hyper pigmentation of the skin, vomiting, diarrhea, cholera and skin, bladder, lungs, kidneys and liver cancers (Nzihou *et al.* (2013), Wang *et al.* (2014)). This injection may also cause an increase in spontaneous abortions, late fetal deaths, prematurity and low birth weight (INERIS, 2014). The most indicators sensitive of chronic exposure to arsenic are cutaneous effects, which are the earliest clinical sign of arsenic poisoning. The optimal arsenic level in drinking water should lie below 0.01 mg/L according to WHO guidelines (OMS, 2004). The works of Mangoua-Allali *et al.* (2015) reported arsenic levels above the WHO threshold value in well water in Akouédo, Côte d'Ivoire. There are several techniques to reduce the arsenic rate of water. However, the most popular are coprecipitation (iron or aluminum salts, lime, oxide of manganese), ion exchange (Ficklin, 1983), reverse osmosis or nanofiltration (Sato *et al.*, 2002) and adsorption. For example, ion exchange is a simple but limited method because it requires filtering the samples to remove suspended solids, the problem of deterioration of the support and the fate of the concentrated waste obtained (Korngold *et al*., 2001). The use of membrane techniques such as reverse osmosis or nanofiltration makes it possible to obtain a very low residual arsenic concentration but requires pre-conditioning of the water to be treated and poses regeneration problems (Clifford & Lin, 1991). The high cost of these methods limits their use. In recent years, adsorption techniques have been quite popular, due to their simplicity as well as the availability of wide range of adsorbents. Removal of pollutants from aqueous environments onto microporous active carbon is a favorite choice because of the highs adsorption capacity (Ziati *et al.*, 2012). However the high cost and irreversible nature of adsorption makes its use limited. Several workers have used a variety of low- cost adsorbents, both natural and synthetic (Chutia *et al*., 2009; Kim *et al.*, 2004). Calcined sandstone and laterite has been used in this study, to remove arsenic. We present firstly, our obtained results on the characterization calcined materials. In the second part, we present results concerning the adsorption of arsenic on these three materials. The extent of adsorption was investigated as a function of contact time, initial concentration and solution pH.

## 2. Material and methods

### 2.1. Adsorbent

In this research, Sandstone and Laterite used are local natural materials collected respectively at Akouedo and Sinematialy in Ivory Coast. These materials were washed several times to remove earthy matter and finally rinsed with distilled water. Then, the samples were crushed and sieved to have a desired particles size (less than 250 μm) using a Saulas NF.X 11.501 sieve.

### 2.1. Adsorbate

Arsenic stock solution was prepared by dissolving reagent-grade As (III) of 99.5% purity into deionized water. Working solutions containing arsenic were prepared by dissolving appropriate amount of arsenic from stock solutions in well water (Nemade *et al.*, 2009). Well water analysis showed that pH varied from 6.3 to 6.6. Experiments were performed at ambient temperatures (25°C).

### 2.2. Effect of Calcination temperature: Optimal temperature

Sandstone and laterite were calcined at different temperatures, such as 300°C, 400°C, 500°C, 600°C and 700°C for 2h, and used to conduct the adsorption of arsenic in a batch at room temperature (25°C). The adsorption process was carried out by using 40 ml of groundwater containing arsenic in a 500 mL glass vials. The glass vials was placed in a speed-controlled stirrer at 200 rpm. Initial arsenic concentrations is 5 mg/L. Adsorbent dosage was 3g of sandstone and 2g of laterite (Koua-Koffi *et al.*, 2018) and pH of water was maintained at 7 by adding $HNO_3$ or NaOH. In order to remove the suspended solid particles, after 24h of adsorption, the treated water was filtered by 0.45 μm cellulosic acetate film. Arsenic concentration was analyzed using an Optical Emission Spectrometer OPTIMA 2100 Dual View (ICP-OES 2100 DV). The arsenic adsorbed percentage was calculated using this relation (1):

$$\% \text{ As (III)adsorbed} = \frac{(C_0 - C_f)}{C_0} * 100 \qquad (1)$$

where $C_0$ and $C_f$ are the initial Arsenic concentration and the final concentration of As in the solution at the time t (mg/L).

### 2.3. Characterization of adsorbent

Calcined sandstone and laterite have been characterised by Fourier Transform Infrared (FTIR) spectroscopy (Bruker Alpha-p) in the spectral range of 400 and 4000 cm$^{-1}$, by X-ray diffraction (XRD) to identify the mineralogical phases, and by thermal analysis (TGA-DSC).

### 2.4. Adsorption studies

### 2.4.1. Adsorption kinetics and effect of initial concentration

The adsorption kinetic study was performed for arsenic in aqueous solution at pH 7 and room temperature (25°C). Several glass vials were used to hold 40 mL arsenic aqueous solution of known initial concentration (1, 5 and 10 mg/L) and 2g of calcined laterite, 3g of calcined sandstone and shaken at 200 rpm for 24 hours. The samples were withdrawn from the shaker at intervals from 15 min to 24 h, filtered and the supernatants were analyzed by Optical Emission Spectrometer OPTIMA 2100 Dual View (ICP-OES 2100 DV). The quantity of arsenic adsorption at any time t, $q_t$ (mg/g), was calculated according to relation (2):

$$q_e = \frac{(C_0 - C_f)}{m} * V \qquad (2)$$

where $C_0$ is the initial As concentration (mg/L), $C_f$ is the final concentration of arsenic in the solution after equilibrium is attained (mg/L), V is the volume of the arsenic solution (L) and m is the weight of the adsorbent (g) used.

### 2.4.2. Effect of pH on Arsenic adsorption

The effect of solution pH was carried out by adding the optimal dose of sorbent in 40 mL of arsenic solution at 5 mg/L. The pH (4.0–10.0) was adjusted by adding a few drops of dilute NaOH or $HNO_3$. pH values were controlled by a pH meter. The mixture was agitated with a shaker for 12 hours at 25°C. The As adsorbed percentage was calculated according to relation (1).

### 2.5. Mathematical modeling of adsorption kinetics

Arsenic adsorption data were analyzed using three kinetic models, the pseudo-first-order, pseudo-second-order kinetic and the intraparticle diffusion models. The first order Lagergren's equation is used to determine the rate of the reaction. The relation (3) is:

$$\log (q_e - q_t) = \log q_e - \frac{K1}{2.303} * t \qquad (3)$$

where $K_1$ = rate constant of adsorption, $q_e$ = amount of solute adsorbed (mg/g) at equilibrium, $q_t$ = amount of solute adsorbed (mg/g ) at any time t and t = time (min). When $\log (q_e - q_t)$ is plotted against t, and $K_1$ could be obtained from the slope of the straight line.

The pseudo-second-order reaction is greatly influenced by the amount of pollutant adsorbed on the material's surface and the amount of pollutant adsorbed at equilibrium. The pseudo second order kinetics may be expressed in a linear form as Ho (2006) relation (4).

$$\frac{t}{qt} = \frac{1}{k_2 q_e^2} + \frac{t}{q_e} \qquad (4)$$

where the equilibrium adsorption capacity ($q_e$), and the second order constants $k_2$ (g/mg.h) can be determined

experimentally from the slope and intercept of plot t/q versus t.

The kinetic experimental results were also fitted to the Weber's intraparticle diffusion model. The rate constants of intra-particle transport ($K_d$) can be calculated from the Weber Morris (1963) equation. The relation (5) is:

$$q(t) = K_d \, t^{0.5} + C \tag{5}$$

Where, q (t)= amount of As adsorbed in mg/g, t = time in minute.

## 2.6. Statistical tests

Statistical tests were performed using the Rstudio 3.2.2 software. The wilcoxon test (non-parametric tests) was applied to examine the variability of materials. The threshold of significance of these different tests is 0.05.

## 3. Results and discussion

### 3.1. Effect of Calcination Temperature on the Adsorption of Arsenic

The adsorption of arsenic using calcined sandstone and laterite at different temperatures ranging from 300 ° C to 700 ° C, showed a high percentage of arsenic removal (Table 1). The arsenic removed from calcined sandstone decreases after 300°C, hence the percentage of adsorption which goes from 99.76% to 80.57% for initial arsenic concentration of 5 mg/L. For calcined laterite, a decrease in the percentage of removal of arsenic after 400°C (99.8% to 85.81%). These results show that calcination at a high temperature reduces the adsorption of arsenic. Its suggested that calcination at a high temperature may affect the physical structure or chemical components of the adsorbent, or both (Valix & Cheung, 2002) and reduce adsorption. Four hundred degrees celsius is the best calcination temperature of laterite and 300°C for Sandstone for the adsorption of arsenic satisfied the WHO standard, which states that the maximum arsenic concentration in drinking water must be lower than 0.010 mg/L. This calcination temperature of laterite is similar to those of Nguyen et al. (2011). However, for these authors, the calcination was made during 4h while our study shows that 2h is sufficient to have the same efficiency from where an ecomony of energy and time. The efficiency of this material at this temperature probably results from the different transformations produced during heating. Ruan & Gilkes observed a good adsorption capacity for calcined laterite at 220°C. This difference in temperature could be explained by the origin of the materials. Indeed, temperatures to achieve transformations in the property of the materials can vary according to the origin of the materials (Issiakou, 2016).

Table 1. Effect of Calcination Temperature on the Adsorption of Arsenic

| Adsorbants | Température de calcination °C | Initial concentration of As (mg/L) | Concentration after treatment (mg/L) | Adsorption percentage (%) |
|---|---|---|---|---|
| Laterite | 300 | 4.23 | 0.030 | 99.286 |
| | 400 | 4.23 | 0.008 | 99.80 |
| | 500 | 4.23 | 0.014 | 99.661 |
| | 600 | 4.23 | 0.095 | 97.754 |
| | 700 | 4.23 | 0.6 | 85.815 |
| Sandstone | 300 | 4.23 | 0.010 | 99.76 |
| | 400 | 4.23 | 0.017 | 99.59 |
| | 500 | 4.23 | 0.021 | 99.484 |
| | 600 | 4.23 | 0.224 | 94.704 |
| | 700 | 4.23 | 0.822 | 80.567 |

## 3.2. Characterization of adsorbents

The mineralogical constitution of calcined sandstone and calcined laterite sample was examined by X-ray diffraction (XRD). As it is shown in figure 1, the calcined laterite contained goethite (its peaks at 4.16 and 2.43 Å), quartz (2.45; 2.27 and 1.67 Å), hematite (2.71; 2.51; 2.20 and 1.69 Å), gibbsite (4.86; 4.37; 3.18; 2.45; 2.39 and 1.98 Å) and kaolinite (7.18; 3.55; 2.51; 2.13; 1.82 and 1.67 Å). These minerals are commonly present in laterites. According to Gidigasu, (1971), the mineralogy of these minerals is linked to its genesis and the laterite of Ivory Coast is derived from the alteration of granite and phylliths. While calcined Sandstone component were goethite (4.98, 2.58 and 1.72 Å), and hematite (2.67, 2.51 and 2.24 Å). The predominant mineral of calcined Sandstone is quartz (4.27; 3.34; 2.46; 2.27; 2.13; 1.98; 1.82 and 1.67 Å).
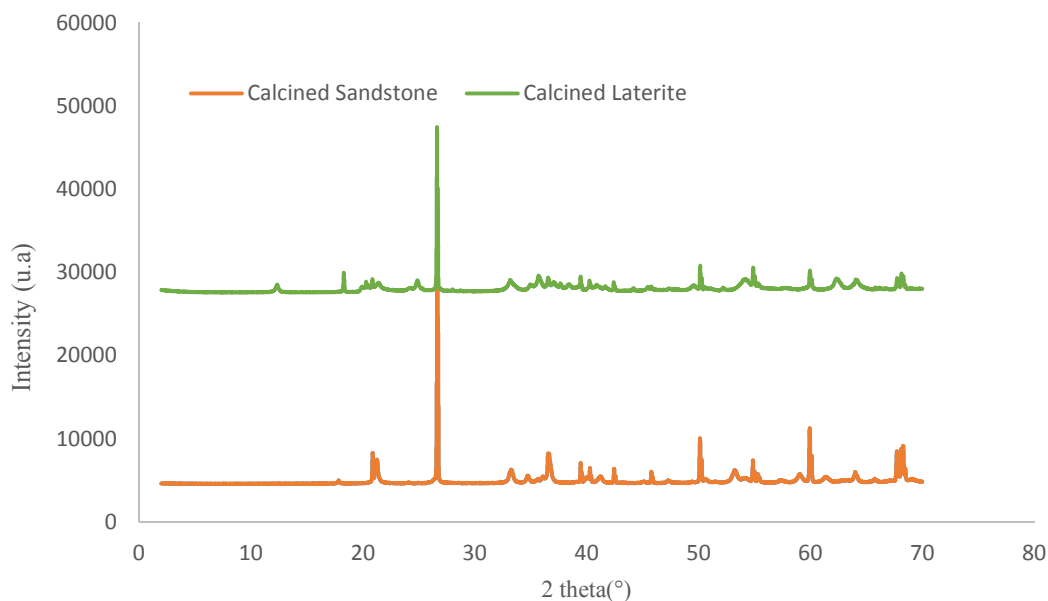
Figure 1. XRD patterns of calcined sandstone and calcined laterite

Figure 2 presented the FTIR spectra of calcined sandstone and calcined laterite in the spectral range of 4000 and 400 cm$^{-1}$. The analysis of the FTIR of calcined laterite (Figure 2b) showed 3695, 3625 and 912 cm$^{-1}$ bands due to the vibrations of the OH and SiO (1117, 1031, 1008 cm$^{-1}$) groups characteristic of kaolinite (Prado *et al.,* 2007). In addition, the bands at 3535; 3469; 3412; 800 and 783 cm$^{-1}$can be attributed to gibbsite. The presence of low intensity bands between 1000 and 2000 cm$^{-1}$. In this interval the bands 2000; 1868 and 1819 cm$^{-1}$ can be attributed to harmonics and combinations of orthosilicates. The adsorbed water and carbonates are respectively represented by the strips 1667 and 1363.

For sandstone (Figure 2a), the 2135 band is thought to be due to the asymmetric elongation vibrations of carbonates related to calcite. The other bands to 1985; 1651, 1654, 1079, 1087, 1042 could be related to the Si-O bonds of quartz and its harmonics (Farmer, 1974, Igisu *et al.*, 2006). The 3185 cm$^{-1}$ band can be attributed to the OH elongation vibrations of the goethite network after Rochester &Topham (1979), Mendelovici *et al.* (1979). As for the band 893 and cm$^{-1}$, it is attributed to the OH deformation vibrations linked to goethite. Bands at 3702; 3695 and 3651 cm$^{-1}$of low intensities are known to be characteristic bands of kaolinite according to Schroeder (2002). Bands at 798; 780; 695 and 696 are characteristic of quartz. And the 695 and 696 band attributable to the Si-O deformation vibration accounts for the crystallinity of the quartz contained in this material (Saika *et al.*, 2008).

Figure 3 shows the TGA-DSC of sandstone and laterite. The treated samples have 3 large areas of distinct mass loss and endothermic peaks: a first loss of mass is about 1.70% for sandstone and 1.44% for laterite. This loss is marked by an endothermic peak that occurs around 52°C and 45°C respectively for sandstone and laterite. The second weight loss is from the order of 0.14% for sandstone, 4.05% for laterite. Endothermic peaks are recorded around 267 °C and 283°C for laterite. This phase, difficult to identify for sandstone, is around 200 ° C. The third loss of mass is 5.10% with a large endothermic peak observed around 493 ° C for laterite. For sandstone, the mass loss is 0.25% and 0.84% respectively. The endothermic peak is around 569°C. Endothermic peaks and loss of mass which marks the departure of hygroscopic and zeolitic water (Carlos *et al.*, 2004), transformation of goethite into hematite by dehydroxylation (Frost & Vassallo, 1996).
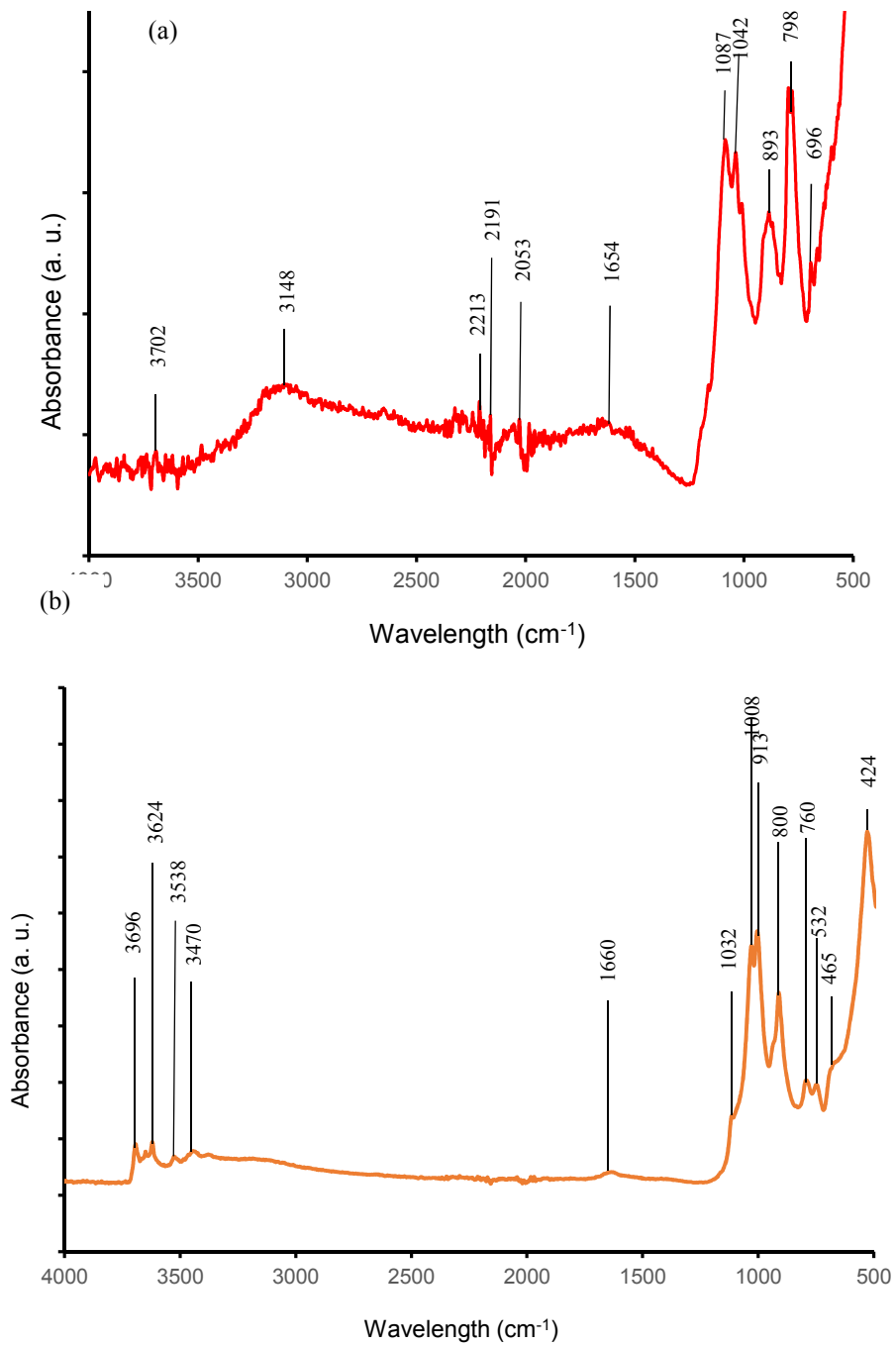
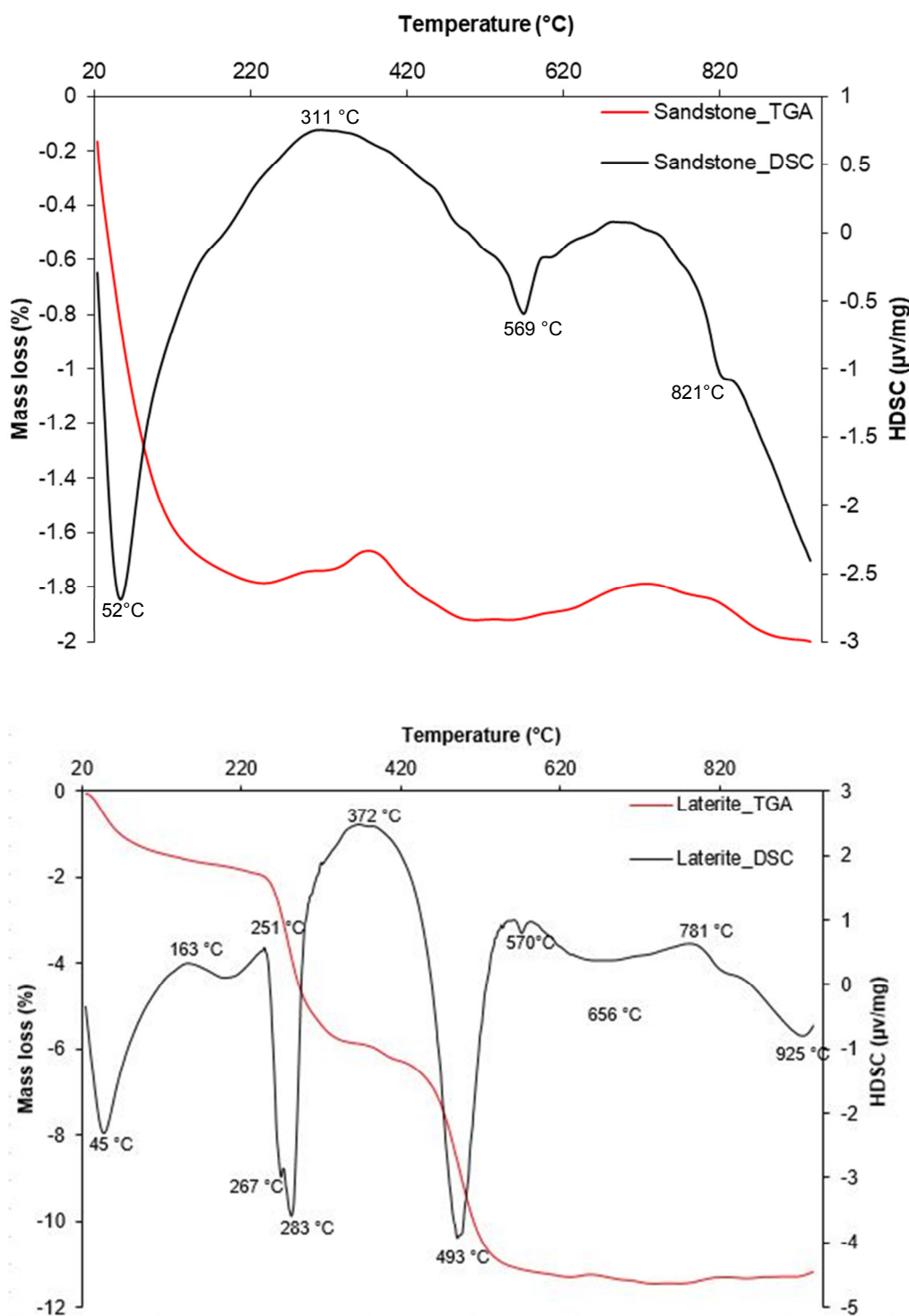Figure 2. FTIR spectra of calcined sandstone (a) and calcined laterite (b)

Figure 3. Analysis Thermogravimetric (TGA) and Differential thermal (DSC) of sandstone and laterite

### 3.3. Effect of contact time and initial concentration

The results of Kinetic studies with different concentrations initial (1-10 mg/L) are shown in Figure 4. As shown in these curves, a rapid arsenic adsorption occurred during the first minutes, indicating an affinity between arsenic and sandstone, shale and laterite surface. This phase would be dependent on easily accessible sites such as external surfaces of particles and macro-pores, or would correspond to the fixation of arsenic ions at the most reactive sites (instant adsorption) (Coulibaly *et al.*, 2016). After approximately 3h and 5 h, the adsorbed amount was stable suggesting a gradual equilibrium respectively from calcined sandstone and laterite. The second phase is slower and stationary, it would be characteristic of a retention of arsenic after diffusion of ions in the meso-

and micropores (gradual adsorption).Therefore a time of 3h and 5 h was chosen for the following experiments concerning calcined sandstone and laterite. Adsorption capacity increases by increasing the initial concentration (1-10 mg/L). The increase in adsorption capacity with the initial concentration could be attributed to the high concentration of arsenic, which provided a greater driving force for the transfer process to overcome mass transfer resistance. A similar observation was made by Sarkar *et al.* (2006) in the interaction of fluoride with crude laterite. The adsorption capacity of arsenic with the calcined materials of this study is greater than that of the same natural materials used by Koua-Koffi *et al.* (2018).The efficiency of calcined adsorbents is probably due to the activation that widened the pore diameter and created new ones. The heating would have induced the appearance of defects in the structure of the material, including voids formed by the departure of the water and the formation of micropores of the nanometer order, associated with the change of volume necessary for the formation of goethites partially dehydroxylated. This mechanism has been demonstrated by Ruan & Gilkes, (1996). Indeed, these authors have shown that partially dehydroxylated goethites are composed of microporous mixtures of goethite and small crystal hematite with a larger surface area so as to promote a high adsorption of arsenic. The amount of arsenic adsorbed on calcined laterite was lesser compared to the other matrix calcined (Test T p <0.05). Laterite had the best efficiency and was followed by sandstone.
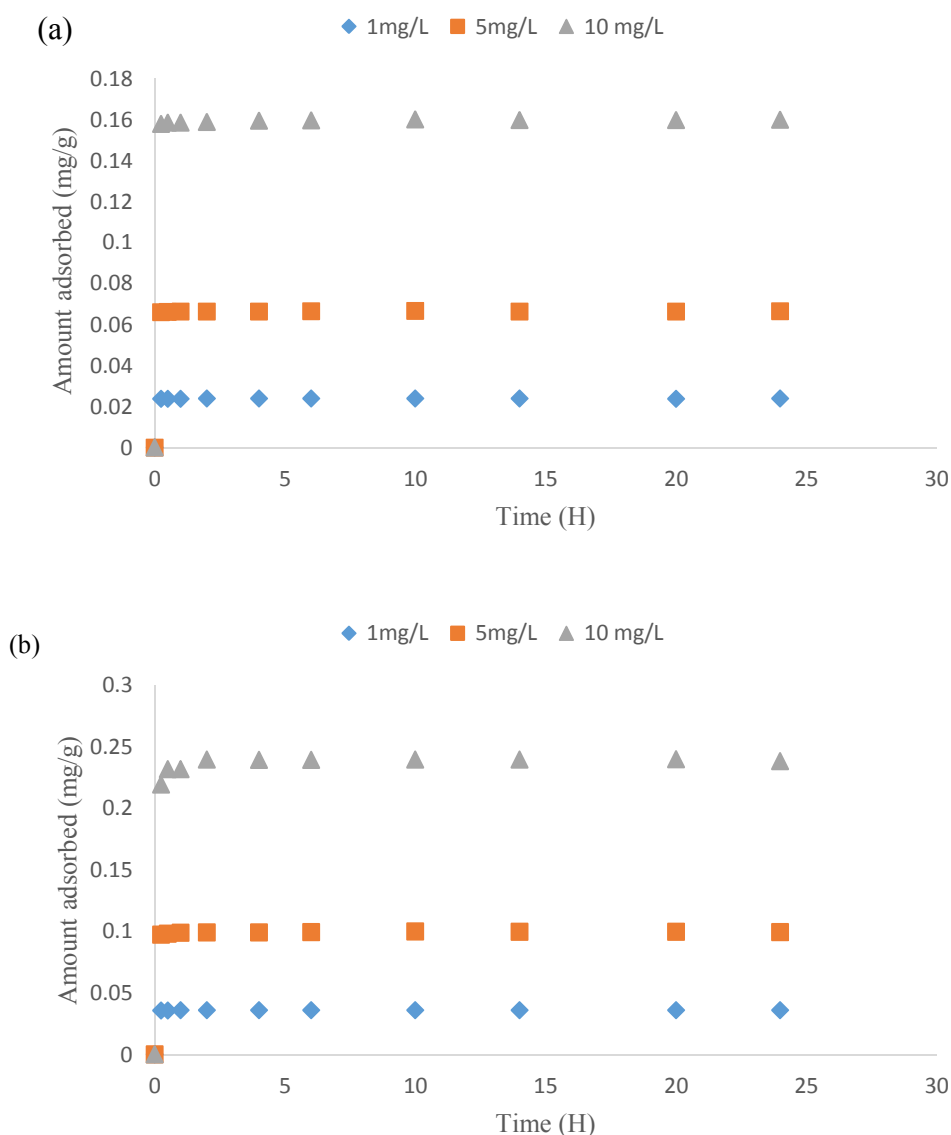


Figure 4. Effect of contact time on the adsorption of Arsenic by calcined sandstone (a) and laterite (b)

## 3.4. Effect of pH

The chemical characteristics of both adsorbent and adsorbate could be varied with pH. The pH of the solution affects the degree of ionization and speciation of various arsenic which subsequently leads to a change in the

kinetics reaction and equilibrium characteristics of the adsorption process. The experimental results for the arsenic adsorption on the calcined materials are shown in Figure 5. The figure shown the adsorption capacities increased with increasing pH. For all adsorbents studied, the optimal pH of adsorption is 6.0. However, with a further increase in pH, percentage removal decreases. The decreases of the percentage can be attributed to the Point of Zero Charge (PZC) of the laterite which is 6.8 and for sandstone is 4.3- 5.6 (Coulibaly *et al*., 2016). At pH higher that the PZC, calcined sandstone and laterite surface is negatively charged and arsenic adsorption becomes less due to repulsion of similar charge, as arsenite exists as anion in that pH range (Maiti *et al*., 2011). Similarly maximum adsorption was observed for As (III) adsorption on iron-oxide coated sand in the pH range 7-7.6 (Gupta *et al*., 2005). Arsenic adsorption at this pH is of the same order as Wilkie & Hering, (1996) where the As (III) adsorption on hydroxide ferric increased with pH up to maximum adsorption at pH 7.
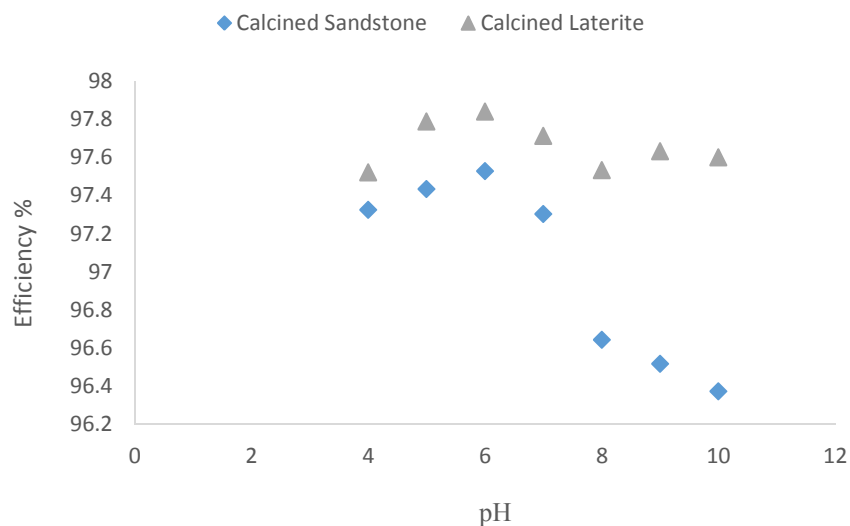


Figure 5. Arsenic removal as a function of pH reactions

### 3.5. Mathematical modeling of adsorption kinetics

The process of arsenic removal from aqueous phase by calcined sandstone and laterite could be modelized by pseudo-first-order kinetics (reversible or irreversible) or pseudo-second-order kinetics and intra-particle diffusion models.

### 3.5.1. Pseudo-first-order model

Figure 6 show the fraction of arsenic adsorbed calculated with the pseudo-first-order. The correlation coefficients for calcined sandstone and laterite are higher than 0.78, and $q_e$ values do not agree with the experimental $q_e$ values (Table 2). This shows that the transfer of arsenic can not be described by a first order law. In other words, the rate of reaction does not depend solely on the concentration of arsenic in solution. which indicates that the adsorption of arsenic is not an ideal pseudo-first-order reaction.
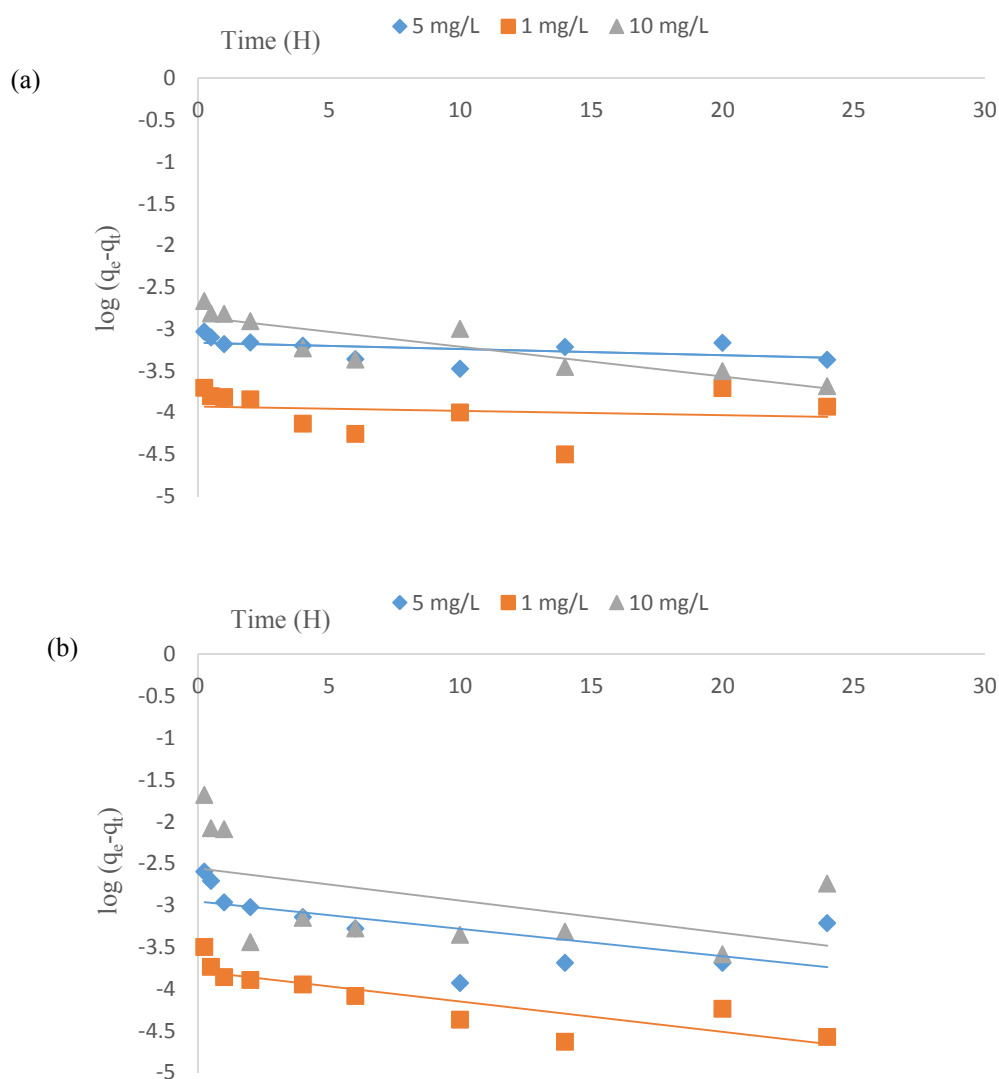
Figure 6. Plots of sorption kinetics of arsenic (III) according to à pseudo-first-order onto calcined sandstone (a) and laterite (b)

### 3.5.2. Pseudo-second-order model

The plot of $t/q_t$ versus t show on Figure 7. For this adsorbents, the calculated values of $K_2$, experimental values of $q_e$ and the corresponding linear regression correlation coefficients R are presented in Table 2. The data showed that the R value of pseudo-second-order model is more than 0.99. More important, the $q_e$ (cal) obtained with the pseudo-second kinetic model, are in agreement with experimental adsorption capacity $q_e$ (exp). The pseudo-second order model describes better the effect of arsenic adsorption by the adsorbents. Conformity to the pseudo-second order model suggests that chemisorption is the dominant mechanism in arsenic retention on the two used laterite. Similar kinetics have been reported by Zehhaf *et al*. (2015) for the adsorption of arsenic on montmorillonite.
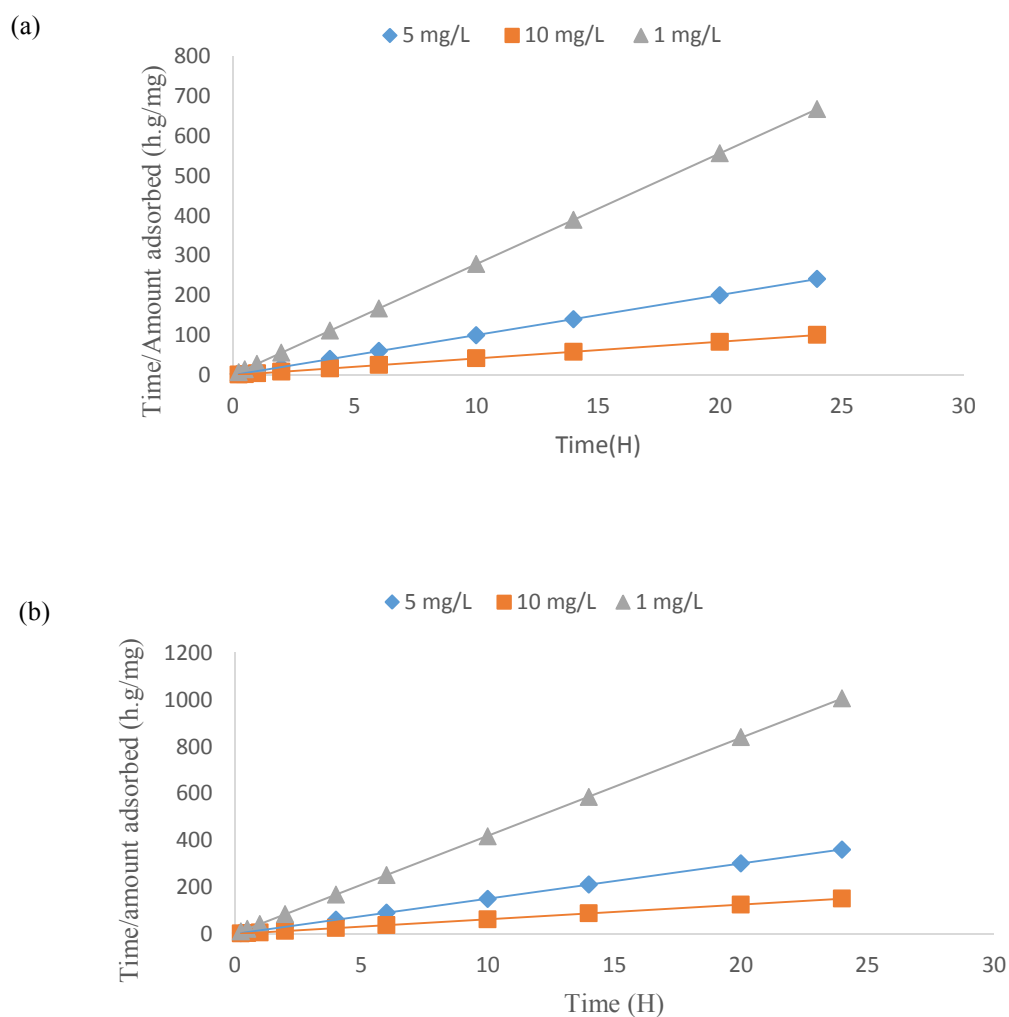
(a)



(b)



Figure 7. Plots of sorption kinetics of arsenic (III) according to à pseudo-second-order onto calcined sandstone (a) and laterite (b)

### 3.4.3. Intra-particle diffusion models

The graphs are plotted between q(t) and $t^{0.5}$ and are shown as Figure 8. $K_d$ the rate constant for intra-particle diffusion are determined from the slopes of the linear portion of the respective plots and are shown in Table 2. The linear portions of the curves do not pass through the origin, indicate that the intraparticle diffusion is not the only rate controlling this step. The Figure 8 shows that only 10 mg/L initial concentration of the materials has two stages. Intraparticule rate constant values ($K_d$) increased with initial As concentration. Concerning, intra particule diffusion, the first stage could correspond to the mass transfer of the adsorbed ions from the bulk solution to the adsorbents surface or instantaneous reactions and the second stage is the intraparticle diffusion on adsorbents (Vaghetti *et al.*, 2009). It is found that those intraparticule rate constant values ($K_d$) increased with initial As concentration. The increase of Kd with the increase of initial As concentration could be explained by the growing effect of driving force which will reduce the diffusion of As species in boundary layer and enhance to diffusion in the solid. Otherwise, the high $K_d$ values of laterite could be related to its high porosity and specific area (Coulibaly *et al.*, 2016).
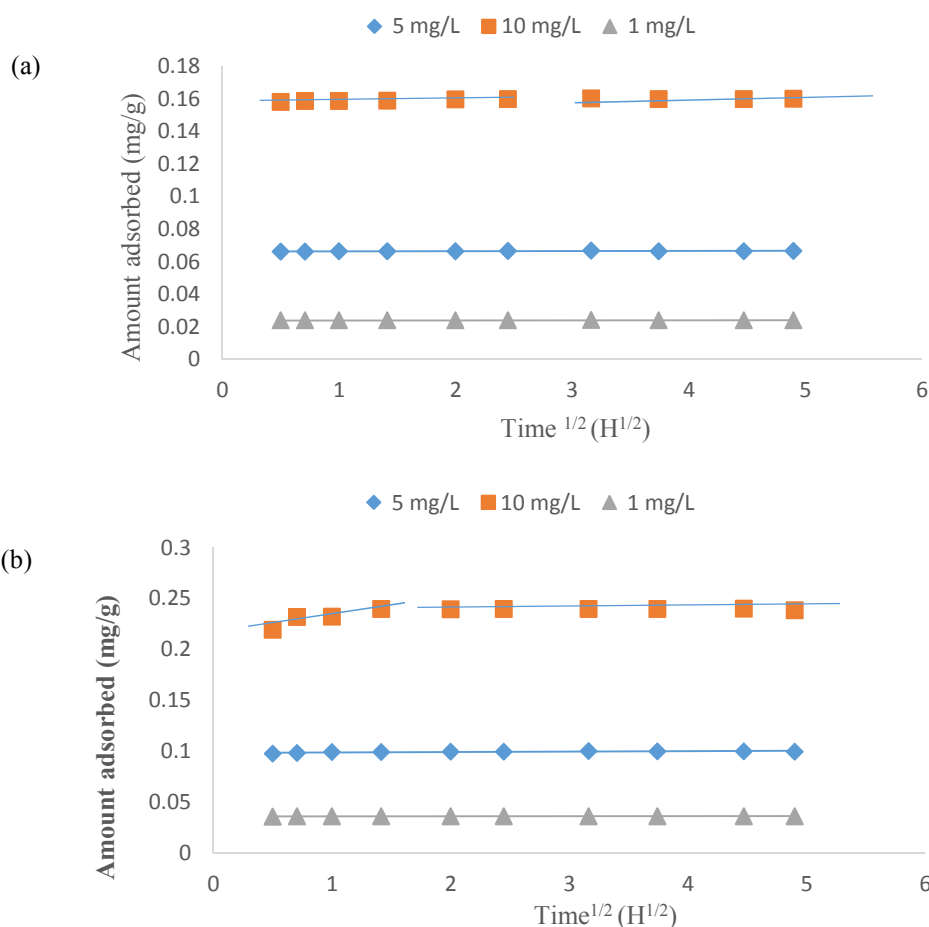
Figure 8. Plots of intra-particule diffusion rate constants for arsenic sorption onto calcined sandstone (a) and laterite (b)

Table 2. Kinetic parameters arsenic adsorption by calcined sandstone and calcined laterite

| | Experimental parameter | | Pseudo-first-order kinetic model | | | Pseudo-second-order kinetic model | | | Intra-particle diffusion model | | |
|---|---|---|---|---|---|---|---|---|---|---|---|
| | $C_o$ (mg As/g) | $q_{e.exp}$ (mg As /g) | $q_{e\,cal}$ (mg As /g) | $k_1$ ($h^{-1}$) | R | $q_{e\,cal}$ (mg As /g) | $k_2$ | R | $k_d$ ($\ast 10^{-3}$ mg/h$^{1/2}$ g) | C | R |
| Laterite | 1 | 0.036 | 0.0226 | 0.0833 | 0.264 | 0.0359 | 6162.903 | 1 | 0.05 | 0.035 | 0.836 |
| | 5 | 0.1 | 0.0519 | 0.0753 | 0.534 | 0.0996 | 3500.167 | 1 | 0.4 | 0.098 | 0.784 |
| | 10 | 0.24 | 0.0773 | 0.0889 | 0.484 | 0.239 | 1606.11 | 1 | 2.703 | 0.229 | 0.645 |
| Sandstone | 1 | 0.0024 | 0.0196 | 0.0117 | 0.171 | 0.0238 | 4091.337 | 1 | 0.01 | 0.023 | 0.326 |
| | 5 | 0.067 | 0.0423 | 0.0173 | 0.4737 | 0.0665 | 11839.227 | 1 | 0.07 | 0.066 | 0.626 |
| | 10 | 0.16 | 0.0575 | 0.0822 | 0.877 | 0.1598 | 962.1705 | 1 | 0.4 | 0.158 | 0.866 |

**Conclusion**

This work focuses on the study of the adsorption capacity of the arsenic on calcined rock particles at different temperatures. Arsenic is inorganic pollutant and highly toxic at high doses. Characterization of our adsorbates showed that the calcination resulted in a change phase. The calcination of sandstone and laterite at 300°C and 400°C during 2h widened the pore diameter and created new ones. She induced the appearance of defects in the

structure of the material. The study of the kinetics was performed in order to understand and explain the arsenic adsorption mechanism on the calcined sandstone and laterite. After calcination of materials, adsorption capacity was increased compared to uncalcined sandstone and laterite. This study follows the pseudo-order model 2, adsorption of arsenic on these materials is likely governed by chemical interactions and then one can conclude, heterogeneity of the binding sites without any interaction between the adsorbed species. This work shows that the calcination of sandstone and laterite is a very interesting optimization setting for the treatment of drinking water polluted with the arsenic.

## References

Carlos, A., Costa, S., Bigham, J-M., Tormena C. A. & Pintro, J. C. (2004). Clay mineralogy and cation exchange capacity of Brazilian soils from water contents determined by thermal analysis. *Thermochimica Acta,* 413, 73-79.

Chutia, P., Shigeru, K., Kijima, T. & Satokawa, S. (2009). Arsenic adsorption from aqueous solution on synthetic zeolites. *J. Hazard Mater,* 162, 440-447

Clifford, D., & Lin, C.-C. (1991). Arsenic (III) and arsenic (V) removal from drinking water in San Ysidro, New Mexico, EPA/600/S2-91/011, U.S. EPA, Cincinnati.

Coulibaly, S. L., Akpo, K. S., Yvon, J. & Coulibaly, L. (2016). Fourier transform infra-red (FTIR) spectroscopy investigation, dose effect, kinetics and adsorption capacity of phosphate from aqueous solution onto laterite and sandstone. *J. Environ. Manage.*, 183, 1032-1040.

Farmer, V. C. (1974). In the infrared spectra of minerals. Edited by V C Farmer, Mineral Society, London; 331p.

Ficklin, W. H. (1983). Separation of arsenic (III) and arsenic (V) in ground waters by ion exchange. *Talanta*, 30, 371-373.

Fields, K., Chen, A. and Wang, L. (2000). Arsenic Removal from Drinking Water by Iron Removal Plants.

Frost, R. L. & Vassallo, A. M. (1996). The déshydroxylation of the kaolinite clay minerals infrared emission spectroscopy. *Clays Clay Miner*., 44 (5), 635-651.

Gidigasu, M. D. (1971). The importance of soil genesis in the engineering classification of Ghana soils. *Eng Geol.* 5, 117-161.

Gupta, V. K., Saini, V. K., & Neeraj, J. (2005). Adsorption of Arsenic (III) from aqueous solutions by iron oxide-coated sand. *Journal of Colloid and Interface Science*, 288, 55-60.

Ho,Y. S. (2006). Review of second-order models for adsorption systems. *J. Hazard. Mater.,* B136,681-689.

Igisu, M., Nakashima S., Ueno Y., Stanley M. Awramiks S. M. & Maruyama S. (2006). In Situ Infrared Microspectroscopy of 850 Million-Year-Old Prokaryotic Fossils. *Applied Spectroscopy* 60 (10), 1111-1121.

INERIS (Institut National de l'Environnement industriel et des Risques), (2010). Fiche de données toxicologiques et environnementales des substances chimiques : Arsenic et ses dérivés inorganiques, 124p.

Kim, Y. H., Kim, C. M., Choi I., Rengaraj, S. &Yi, J. H. (2004). Arsenic removal using mesoporous alumina prepared via a templating method. *Environ Sci Technol* 38:924–931.

Korngold, E., Belayev N., & Aronov, L. (2001). Removal of arsenic from drinking water by anion exchangers. *Desalination,* 141, 81-84.

Koua-Koffi, N., Coulibaly, L., Sangare D. & Coulibaly, L. (2018). Laterite, Sandstone and Shale as Adsorbents for the Removal of Arsenic from Water. *American Journal of Analytical Chemistry*, 9 (7), 340-352. doi: 10.4236/ajac.2018.97027.

Maiti, A., Jayanta, K. B. & Sirshendu, D. (2011). Chemical treated laterite as promising fluoride adsorbent for aqueous system and kinetic modelling. *Desalination*, 265 (1-3), 28-36.

Mangoua-Allali, A. L. C., Koua-Koffi, A., Akpo, K. S. & Coulibaly, L. (2015). Evaluation of Water and Sanitation Situation of Rural Area near Landfill, Abidjan. *Journal of Chemical, Biological and physical sciences*, 5 (3), 3033-3041.

Mendelovici, E., Yariv, S. H. & Villalba R. (1979). Aluminum-bearing goethite in Venezuelan laterite. *Clays and Clay Miner.,* 27 (5), 368-372.

Nemade P. D., Kadam A. M. & Shankar H. S. (2009). Adsorption of arsenic from aqueous solution on naturally available red soil. *Journal of Environmental Biology*, 30(4), 499-504.

Nguyen, P. T. N., Abella, L. C., Gaspillo, P. D. & Hinode, H. (2011). Removal of arsenic from simulated groundwater using calcined laterite as the adsorbent. *Journal of chemical engineering of Japan,* 44 (6), 411 - 419.

Nzihou, J. F., Bouda, M., Hamidou, S. & Diarra, J. (2013). Arsenic in Drinking Water Toxicological Risk Assessment in the North Region of Burkina Faso. *Journal of Water Resource and Protection*, 5, 46-52. doi.org/10.4236/jwarp.2013.58A007.

OMS (2004). Fluoride and arsenic in drinking water. Inheriting the World: The Atlas of Children's Health and the Environment. www.who.int/water_sanitation_health/en/poster8, (17/02/2015), 33p.

Prado, B., Duwig, C., Hidalgo, C., Gômez, D. & Yee, H. (2007). Characterization, functioning and classification

of two volcanic soil profiles under different land uses in Central Mexico. *Geoderma*, 139, 300-313. http://dx.doi.org/10.1016/j.geoderma.2007.02.000.

Rochester, C. H. & Topham, S. A. (1979). Infrared study of surface hydroxyl groups on goethite. *J.C.S. Faraday I.*, 75, 591-602.

Ruan, H. D. & Gilkes, R. J. (1996). Kinetics of phosphate sorption and desorption by synthetic aluminous goethite before and after thermal transformation to hematite. *Clays Clay Miner.*, 31 (1).

Sarkar, M., Banerjee, A., Pramanick, P. P. & Sarkar, A. R. (2006). Use of Laterite for the Removal of Fluoride from Contaminated Drinking Water. *J. Colloid Interface Sci.,* 302, 432-441.

Sato, Y., Kang, M., Kamei, T. & Magara, Y. (2002). Performance of nanofiltration for arsenic removal. *Water Research*, 36, 3371-3377.

Schroeder, P. A. (2002). Infrared Spectroscopy in clay science: In CMS Workshop Lectures, 11, Teaching Clay Science, A. Rule and S. Guggenheim, eds., The Clay Mineral Society, Aurora, CO, 181-206.

Vaghetti, J. C. P., Lima, E. C., Royer, B., Cardoso, N. F., Martins, B. & Calvete, T. (2009). Pecan nutshell as biosorbent to remove toxic metals from aqueous solution. *Separation Science and Technology*, 44, 615-644.

Valix, M. & Cheung, W. H. (2002). Study of Phase Transformation of Laterite Ores at High Temperature. *Min. Eng.* 15, 607-612

Wang, C., Luo, H., Zhang, Z., Wu, Y., Zhang, J. & Chen, S. (2014). Removal of As (III) and As (V) from aqueous solutions using nanoscale zero valent iron-reduced graphite oxide modified composites. *J. Hazard Mater,* 268, 124-131.

Weber W. J., & Morris J. C. (1963). Kinetics of adsorption on carbon from solution. *J. Sanit. Eng. Div. Am. Soc. Civ. Eng.* 89, 31-60.

Welté, B. & Montiel, A. (2004). Traitements d'élimination de l'arsenic, du sélénium et de l'antimoine. Journée d'échanges, BRGM Orléans, 24p.

Wilkie, J. A. & Hering, J. G. (1996). Adsorption of arsenic onto hydrous ferric oxide: Effects of adsorbate/adsorbent ratios and co-occurring solutes. *Colloids Surf A Physicochem. Eng. Asp.,* 107, 97-110.

Zehhaf, A., Benyoucef, A., Quijada Tomás, C., Taleb, S. & Morallón, E. (2015). Algerian natural montmorillonites for arsenic (III) removal in aqueous solution. *International Journal of Environmental Science and Technology*, 12 (2), 595-602.

Ziati, M., Hazourli, S., Nouacer, S., & Khelaifia, F. Z. (2012). Elimination of arsenic (III) by adsorption on coal resulting from date pits and activated thermally and chemically. *Water Quality Research Journal of Canada,* 47 (1), 91-102.